

## Electrocatalytic activity of cobalt tris(4-nitrophenyl)corrole for hydrogen evolution from water

Hai Chen, Dong-Lan Huang, Md Sahadat Hossain, Guo-Tian Luo & Hai-Yang Liu

To cite this article: Hai Chen, Dong-Lan Huang, Md Sahadat Hossain, Guo-Tian Luo & Hai-Yang Liu (2019): Electrocatalytic activity of cobalt tris(4-nitrophenyl)corrole for hydrogen evolution from water, Journal of Coordination Chemistry, DOI: [10.1080/00958972.2019.1671588](https://doi.org/10.1080/00958972.2019.1671588)

To link to this article: <https://doi.org/10.1080/00958972.2019.1671588>

 View supplementary material [↗](#)

 Published online: 01 Oct 2019.

 Submit your article to this journal [↗](#)

 Article views: 17

 View related articles [↗](#)

 View Crossmark data [↗](#)



# Electrocatalytic activity of cobalt tris(4-nitrophenyl)corrole for hydrogen evolution from water

Hai Chen<sup>a,b</sup>, Dong-Lan Huang<sup>b</sup>, Md Sahadat Hossain<sup>b</sup>, Guo-Tian Luo<sup>a</sup> and Hai-Yang Liu<sup>b</sup>

<sup>a</sup>College of Chemistry and Chemical Engineering, Gannan Normal University, Ganzhou, China;

<sup>b</sup>Department of Chemistry, The Key Laboratory of Fuel Cell Technology of Guangdong Province, South China University of Technology, Guangzhou, China

## ABSTRACT

Catalytic activities for hydrogen ( $H_2$ ) evolution of cobalt 5,10,15-tris(phenyl)corrole (**1**) and 5,10,15-tris(4-nitrophenyl)corrole (**2**) (in homogeneous system) was examined from acetic acid and water. In phosphate buffer solution (pH 7.0), the hydrogen evolution turnover frequency (TOF) for **1** and **2** were 62 and  $150\text{ h}^{-1}$  at the overpotential of  $-1.53\text{ V}$  versus Ag/AgCl. In acetic acid media, hydrogen evolution TOF for **1** and **2** were 56 and  $127\text{ h}^{-1}$ , respectively, at an overpotential of 961 mV versus Ag/AgNO<sub>3</sub>. In the practical electrocatalytic hydrogen evolution experiment at  $-1.45\text{ V}$  (vs. Ag/AgCl) overpotential for 1 h, the TOF were 76 and  $188\text{ h}^{-1}$  for **1** and **2**, respectively. No observable decomposition of the catalyst could be observed after electrolysis for 72 h with a glassy carbon electrode.

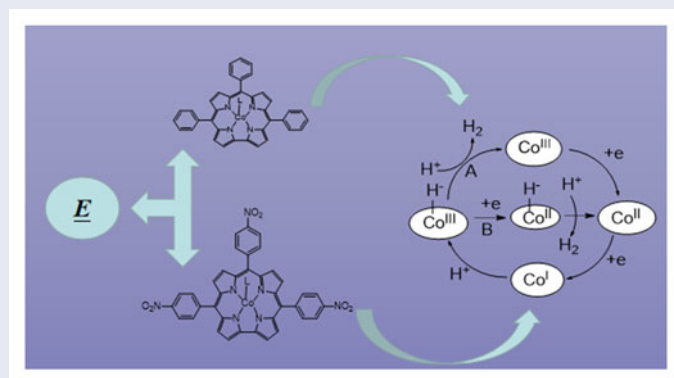
## ARTICLE HISTORY

Received 29 January 2019

Accepted 5 September 2019

## KEYWORDS

Corrole; cobalt; hydrogen evolution; electrocatalysis



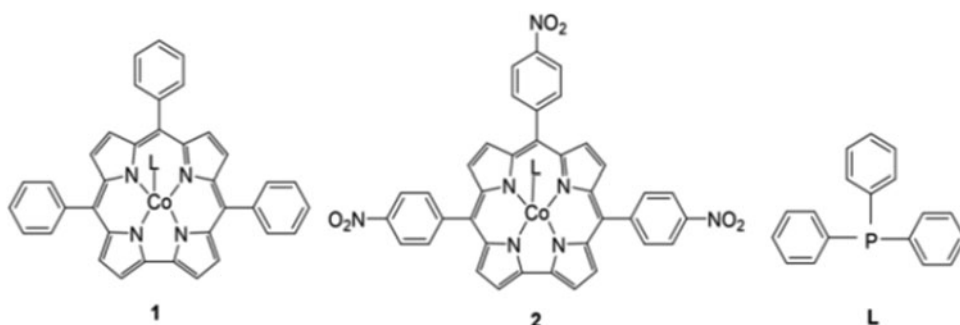
## 1. Introduction

Development of renewable carbon-free energy is a major scientific and technological challenge to meet the energy needs for the future [1]. Hydrogen ( $H_2$ ) is considered as an ideal energy carrier for our future power plants [2, 3]. One common approach to generate  $H_2$  is

CONTACT Guo-Tian Luo  luogt@gnnu.edu.cn; Hai-Yang Liu  chhyliu@scut.edu.cn

 Supplemental data for this article can be accessed here.

© 2019 Informa UK Limited, trading as Taylor & Francis Group



**Scheme 1.** Molecular structure of cobalt corroles.

the water splitting by electrochemical catalysis [4]. In nature, hydrogenase enzymes efficiently catalyze hydrogen evolution. However, these enzymes are difficult to obtain and their stabilities limit the application outside living systems [5]. Some platinum-based catalysts can efficiently catalyze  $H_2$  production from water, but cannot be widely applied because of its low natural abundance [6]. So, there is great demand in searching for hydrogen evolution catalysts of cheap metals. Many cheap metals such as iron [7], copper [8], and cobalt [9] are capable of electrocatalytic hydrogen evolution.

Metallocorroles have been applied in catalytic oxidation [10], azacyclopropaneization [11], and cycloaddition [12] reactions. However, the reports on the application of metal corrole as electrocatalysts for  $H_2$  generation are so far limited to cobalt, copper, and manganese complexes [13]. In 2014, Gross [14] reported that cobalt  $\beta$ -halogenated tris(pentafluorophenyl)corrole could efficiently electrocatalyze hydrogen evolution in acetonitrile solutions. Cao [15] also used cobalt tris(pentafluorophenyl)corrole to catalyze both water oxidation and proton reduction by coating it onto indium tin oxide (ITO) electrodes in aqueous solutions, and found manganese corrole was unstable in the electrocatalytic hydrogen evolution reaction (HER). Copper 5,15-pentafluorophenyl-10-(4-nitrophenyl)corrole was also found active in electrocatalytic  $H_2$  evolution by using trifluoroacetic acid as the proton source in acetonitrile [16]. Recently, we found that electron-deficient cobalt tris(ethoxycarbonyl)corrole exhibited good performance in the HER [17]. Electron-withdrawing substituents can lower the overpotential significantly in the cobalt corrole electrocatalyzed HER [15]. Similar observation was also found in the catalytic oxygen reduction [18]. Nitrophenyl is an electron-withdrawing substituent that may significantly tune chemical and physical properties of corrole derivatives [19]. Redox potentials of cobalt corrole would be positively shifted (easier reduction and harder oxidation) after attaching nitrophenyl substituents [20]. In 2001, Paolesse [21] reported the first synthesis of tris(4-nitrophenyl)corrole. Since then, study on the electrochemical property of its manganese complex [22], crystal structure of its copper complex [23], and its (nitrosyl) iron complex [24] have also been reported. In 2017, Doctorovich [25] used cobalt tris(4-nitrophenyl)corrole doped carbon nanotubes for photocatalytic and photo-electrocatalytic hydrogen production. HER may be achieved at very low overpotential with high efficiency, demonstrating cobalt tris(4-nitrophenyl)corrole is a promising catalyst for hydrogen evolution. How about the electrocatalytic HER performance of this catalyst in homogeneous solution? Here we report the electrocatalytic activity of cobalt 5,10,15-tris(phenyl)corrole (**1**) and cobalt 5,10,15-tris(4-nitrophenyl)corrole (**2**) (Scheme 1) in HER.

Water can be used as a proton source in acetonitrile-water ( $v/v = 2/3$ ) solvent system and **2** exhibits better performance than **1**.

## 2. Experimental

### 2.1. Materials and measurements

All reagents were purchased from commercial sources and used without purification. High resolution mass (HRMS) spectra were obtained with a Bruker Maxis impact mass spectrometer incorporated with an electrospray ionization (ESI) source.  $^1\text{H-NMR}$  spectra were recorded with a Bruker Avance III 400 MHz spectrometer in  $\text{CDCl}_3$  ( $d = 7.26$  ppm) solvent. UV-visible spectra were measured with a Hitachi U-3010. Cyclic voltammograms (CVs) were recorded with a CHI-660E electrochemical analyzer under nitrogen. In the three-electrode cell in which a glassy carbon electrode (1 mm in diameter) was used as the working electrode, saturated  $\text{Ag/AgNO}_3$  (in DMF solution) and  $\text{Ag/AgCl}$  (in buffer solution) as the reference electrode, and a platinum wire as the auxiliary electrode. The supporting electrolyte was 0.1 M  $[(n\text{-Bu})_4\text{N}]\text{ClO}_4$ .

Controlled-potential electrolysis (CPE) experiments were carried out by employing an airtight glass double-compartment cell which was separated by a glass frit in aqueous medium. The working compartment was fitted with a glassy carbon plate and a  $\text{Ag/AgCl}$  reference electrode. The auxiliary compartment was fitted with a platinum gauze electrode. The working compartment was filled with 40 mL of 0.25 M buffer solution (acetonitrile/water (2:3 = V/V) as solvent) containing 0.1 M KCl (supporting electrolyte), the auxiliary compartment was also filled with 40 mL of phosphate buffer solution (pH 7.0). Both compartments were sparged for 60 min with nitrogen. CPE experiments were performed immediately after adding suitable concentration of complex. After electrolysis,  $\text{CH}_4$  was added to the reactor as the internal standard, and the gas mixture was analyzed by using an Agilent Technologies 7890A GC chromatograph.

### 2.2. Preparation of the cobalt complexes

Complexes **1** and **2**: 5,10,15-tris(phenyl)corrole [26] (13.2 mg, 0.025 mmol),  $\text{Co(OAc)}_2 \cdot 4\text{H}_2\text{O}$  (30 mg, 0.12 mmol), and triphenylphosphine ( $\text{PPh}_3$ ) (50 mg, 0.191 mmol) were dissolved in ethanol (20 mL) and the solution was stirred for 1.5 h at room temperature. Dichloromethane (DCM, 50 mL) was then added to the reaction mixture. The mixture was washed three times with water, the organic phase was collected and the solvent was removed by rotary evaporation to obtain the crude product. The product was purified by column chromatography using DCM/Hex ( $V/V = 2/1$ ) as eluent. Recrystallization from DCM/hexane afforded **1** as a red-brown solid (9 mg, yield 75%). Complex **2** was synthesized by the same procedure using 5,10,15-tris(4-nitrophenyl)corrole [21]. HRMS spectra of the complexes are given in the [Supplementary materials](#) (Figures S9 and S10).

Complex **1**: UV-Vis ( $\text{CH}_2\text{Cl}_2$ )  $\lambda_{\text{max}}$  (relative intensity) 384 (1.00), 560 (0.20).  $^1\text{H-NMR}$  (400 MHz,  $\text{CDCl}_3$ ): 8.61 (d, 2H), 8.34 (d, 2H), 8.16–7.97 (m, 7H), 7.68–7.49 (m, 11H), 7.39 (d, 1H), 7.06 (t, 3H), 6.71 (t, 6H), 4.84–4.66 (m, 6H). HRMS, calcd for  $\text{C}_{55}\text{H}_{38}\text{CoN}_4\text{P}$ : 845.2230, found for  $\text{C}_{55}\text{H}_{38}\text{CoN}_4\text{P}$ : 845.2239.

Complex **2**: UV-Vis ( $\text{CH}_2\text{Cl}_2$ )  $\lambda_{\text{max}}$  (relative intensity) 372 (1.00), 575 (0.13).  $^1\text{H-NMR}$  (400 MHz,  $\text{CDCl}_3$ ): 8.79 (d, 2H), 8.44 (m, 8H), 8.12 (d, 2H), 8.04 (d, 2H), 7.95 (d, 4H), 7.78 (d, 2H), 7.18 (t, 5H), 6.96 (t, 10H). HRMS, calcd for  $\text{C}_{55}\text{H}_{35}\text{CoN}_7\text{O}_6\text{P}$ : 980.1770, found for  $\text{C}_{55}\text{H}_{35}\text{CoN}_7\text{O}_6\text{P}$ : 980.1791.

### 3. Results and discussion

#### 3.1. Cyclic voltammetry

Cyclic voltammograms (CVs) of **1** and **2** in DMF are shown in Figure 1. The first ( $E_{1/2} = -0.51\text{ V vs. Ag/AgNO}_3$ ) and second ( $E_{1/2} = -1.65\text{ V vs. Ag/AgNO}_3$ ) redox processes of **1** are reversible, assigned to the  $\text{Co}^{\text{III/II}}$  and  $\text{Co}^{\text{II/I}}$  couples, respectively. Complex **2** exhibits three reversible redox peaks with  $E_{1/2}$  at  $-1.75$ ,  $-1.02$ , and  $-1.53\text{ V vs. Ag/AgNO}_3$ ; these redox signals could be assigned to  $\text{Co}^{\text{II/I}}$ , nitrophenyl group redox [19a], and  $\text{Co}^{\text{III/II}}$  couples, respectively.

The peak current corresponding to cobalt reduction potentials increases with the scanning rate (Supplementary material, Figure S1). The peak current is linear to the square root of the scanning speed. This indicates that the reduction is a diffusion controlled process [2]. The  $\text{Co}^{\text{II/I}}$  reduction current of **2** increased more quickly than **1** with the increase of scanning speed. This suggests diffusion rate of **2** is larger than that of **1** in DMF.

#### 3.2. Catalytic hydrogen evolution in DMF

To determine the electrocatalytic activity of **1** and **2**, we recorded CVs in DMF in the presence of acetic acid. For **1**, adding different amounts of HOAc triggers catalytic currents at potentials near the  $\text{Co}^{\text{II/I}}$  couple (Figure 2(a)). A systematic increase was observed at  $-1.65\text{ V versus Ag/AgNO}_3$  with increasing acid concentrations from 0.00 to 2.20 mM as shown in Figure 2(a). This increase in current can be ascribed to catalytic generation of  $\text{H}_2$  from acetic acid [27]. The onset of the catalytic wave transfers to more anodic values with sequential increments of acid concentration. During addition

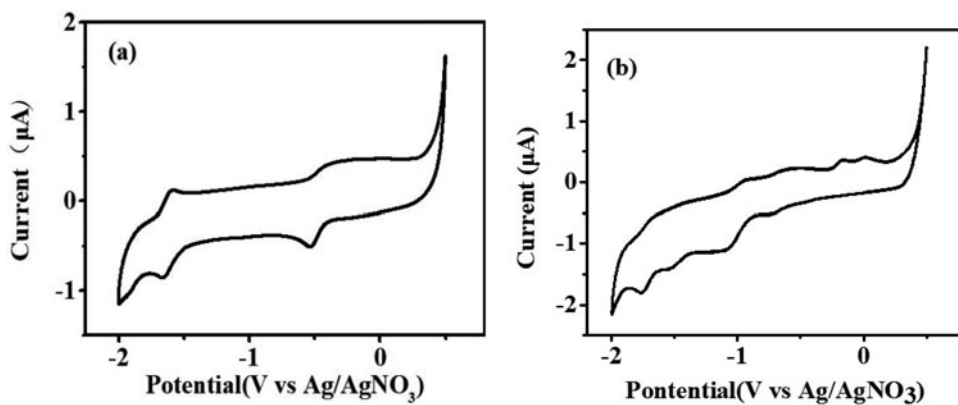


**Figure 1.** Cyclic voltammogram of **1** (a) and **2** (b) (1.15 mM) in DMF solution (0.1 M  $[\text{n-Bu}_4\text{N}]\text{ClO}_4$ , scan rate of 100 mV/s).

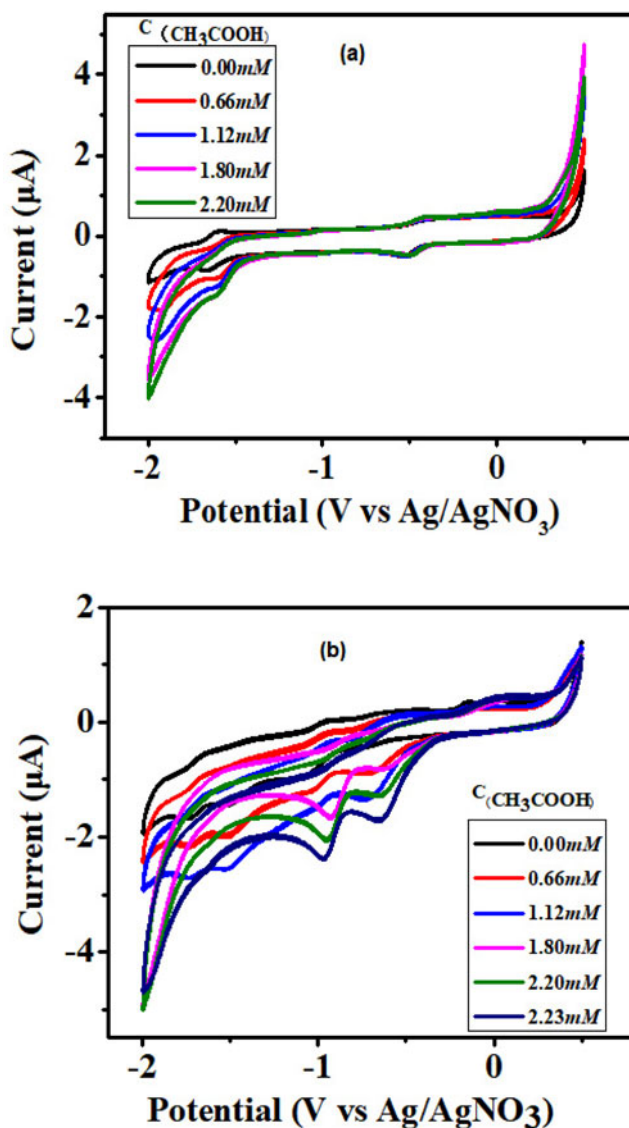
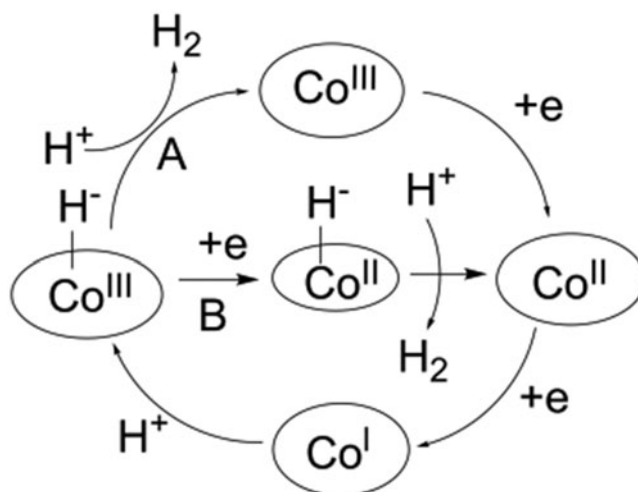


**Figure 2.** CVs of **1** (a) and **2** (b) (1.15 mM) in the absence of acid (black trace) and with different concentrations of acid in DMF. Conditions: room temperature, 0.1 M  $[n\text{-Bu}_4\text{N}]\text{ClO}_4$  as supporting electrolyte, scan rate = 100 mV/s GC working electrode (1 mm diameter), Pt counter electrode, and Ag/AgNO<sub>3</sub> reference electrode.

of HOAc a new hydrogen evolution peak can be observed near  $-1.91\text{ V versus Ag/AgNO}_3$ . Similar observations have been reported for other catalytic systems [28]. As in these examples, hydrogen evolution may also form a cobalt-hydride  $\text{H-Co}^{\text{III}}$  intermediate, formed by the reduction of cobalt  $\text{Co}^{\text{I}}$  specie. Thus there might be two hydrogen evolution pathways A and B in the current catalytic system (Scheme 2). For **2** we can see (Scheme 2) the mechanism of hydrogen production is similar to that of **1**, but since there is no new peak with increase of acidity, the hydrogen production path has no B pathway, but we can see that at  $-1.02\text{ V versus Ag/AgNO}_3$  will change with the



**Scheme 2.** Possible mechanistic pathways for H<sub>2</sub> evolution electrocatalyzed by complexes.

increase of acidity, in [Figure 2\(b\)](#), indicating that the p-nitrophenyl group is also involved in hydrogen production. Combined with previous work [29], the electron transfer in the catalytic process may be on the cobalt or on the ligand transfer. Combined with the research of our group's corrole complex electrocatalytic hydrogen production, electron transfer is on cobalt because electron transfer is unstable on the ligand [17].

A number of control experiments were also conducted under the same experimental conditions to confirm that **1** and **2** are responsible for the catalytic hydrogen evolution, including the metal-free compound, Co(OAc)<sub>2</sub>·4H<sub>2</sub>O and the mixture of the free ligand and Co(OAc)<sub>2</sub>·4H<sub>2</sub>O. As shown in [Figures S3–S6 \(Supplementary material\)](#), the catalytic waves observed for the metal-free compound, Co(OAc)<sub>2</sub>·4H<sub>2</sub>O, or the mixtures of the compound and Co(OAc)<sub>2</sub>·4H<sub>2</sub>O, did not match with **1** and **2**.

Furthermore, bulk electrolyses of a DMF solution with acetic acid at different applied potential in a double-compartment cell were conducted to validate the electrocatalytic activities of **1** and **2**. [Figure 3\(a,c\)](#) shows the charge build up for bulk electrolysis of solutions containing **1** and **2** in the presence of acetic acid. The charge increased when the applied potential was increased. Another way to analyze good catalytic efficiency is that catalysis could occur with relatively low overpotential. The overpotential is defined by [Equation \(1\)](#) [30]; from [Figure 3\(a\)](#), we can see that when the overpotential was 391 mV versus Ag/AgNO<sub>3</sub>, catalysis occurred. Further, when the applied potential was −1.45 V versus Ag/AgNO<sub>3</sub>, the maximum charge reached 64.9 mC during 2 min of electrolysis,

$$\begin{aligned} \text{Overpotential} &= \text{Applied potential} - E_{HA}^0 \\ E_{HA}^0 &= E_{H^+}^0 - (2.303RT/F)pK_{aHA} \end{aligned} \quad (1)$$

where  $E_{H^+}^0$  is the standard potential for the solvated proton-dihydrogen couple and  $K_{a,HA}$  is the dissociation constant of acetic acid.

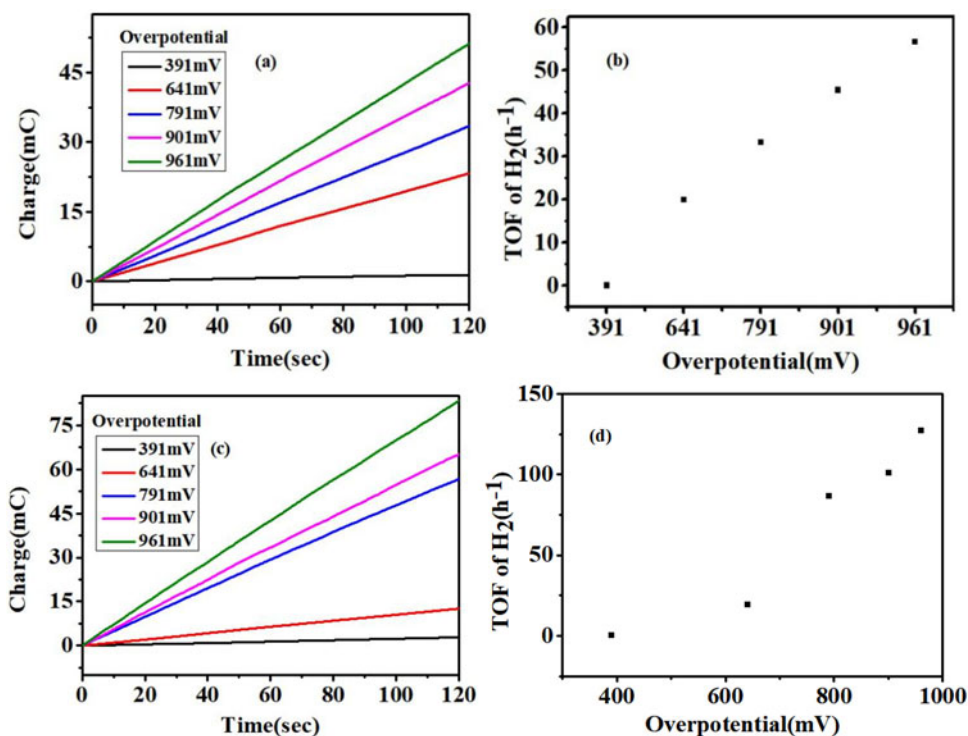


**Figure 3.** Charge buildup vs. time from electrolysis of **1** (a) and **2** (c) (0.005  $\mu$ M) in DMF (0.1 M [n-Bu<sub>4</sub>N]ClO<sub>4</sub>) under different overpotentials. All data have been processed by blank subtraction. Turnover frequency (mol H<sub>2</sub>/mol catalysts/h) for electrocatalytic hydrogen production by **1** (b) and **2** (d) (0.005  $\mu$ M) under overpotentials (mV vs. Ag/AgNO<sub>3</sub>).

Presuming every catalyst molecule and every electron are used for the reduction of protons, according to Equation (2) [31], we measured TOF values for the catalysts reaching a maximum of 56 and 127 h<sup>-1</sup> at an overpotential of 961 mV (Supplementary material, Equations (S1) and (S2)) for **1** (b) and **2** (d), respectively. Hence, the two complexes have similar catalytic capacities, with **2** better than **1**,

$$TOF = \Delta C / (F \times n_1 \times n_2 \times t) \quad (2)$$

where  $\Delta C$  is the charge from the catalyst solution during CPE minus the charge from solution without catalyst during CPE,  $F$  is Faraday constant,  $n_1$  is the moles of electrons required to generate 1 mol of H<sub>2</sub>,  $n_2$  is the moles of catalyst in solution, and  $t$  is the duration of electrolysis.

### 3.3. Catalytic hydrogen evolution in aqueous media

We also studied catalytic hydrogen evolution in aqueous media, a more attractive hydrogen power generation sustainable medium. CVs were carried out in 0.25 M phosphate buffers at different concentrations. At pH 7, the catalytic current was not apparent until a potential of  $-1.31$  V versus Ag/AgCl was attained in the absence of **2** (Figure 4(c)). With addition of **2**, the onset of catalytic current was observed at about  $-1.32$  V versus Ag/AgCl, and the current increased significantly with increasing

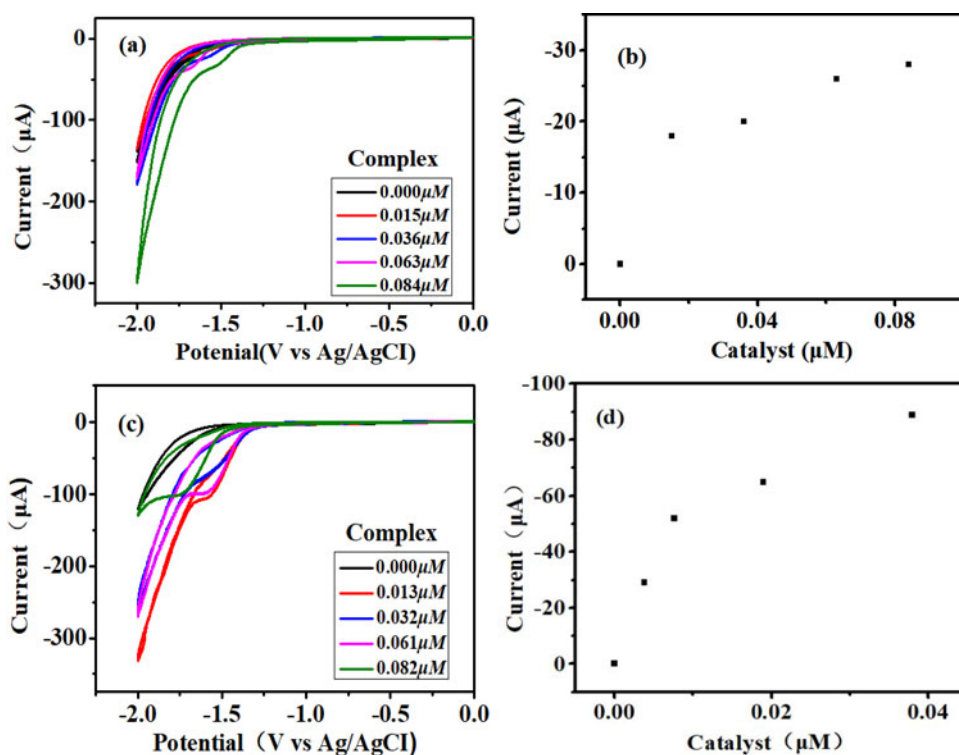


**Figure 4.** CVs of **1** (a) and **2** (c) at different concentrations (pH = 7.0). Conditions: 0.1 M KCl as supporting electrolyte; scan rate,  $100 \text{ mV s}^{-1}$ ; GC working electrode (1 mm in diameter); Pt counter electrode; Ag/AgCl reference electrode. Plot of catalytic peak current vs. concentrations of **1** (b) and **2** (d).

concentrations of **2** from 0.00 to  $0.082 \mu\text{M}$ . The potential shifted to the positive value of about 380 mV compared to that in the absence of **2**, indicating that **2** can catalyze the reduction of protons from water to  $\text{H}_2$ . Catalytic hydrogen production can also be achieved with **1** in neutral buffer (Figure 4(a,b)).

Figure 5(a,c) shows the bulk electrolysis in aqueous media at different applied potential in a double-compartment cell. The total charge for bulk electrolysis of solutions containing **1** and **2** increased when the applied potential was added. Based on Equation (2), the TOF for **1** was  $62 \text{ h}^{-1}$  at an overpotential of  $-1.53 \text{ V}$  versus Ag/AgCl (pH 7.0) (see Supplementary material, Equation (S3) and Figure 5(b)). Based on Equation (2), the TOF for **2** was  $150 \text{ h}^{-1}$  at an overpotential of  $-1.53 \text{ V}$  versus Ag/AgCl (pH 7.0) (see Supplementary material, Equation (S4) and Figure 5(d)). Comparing the two results, **2** is a better catalyst than **1**; also the TOF of **2** is higher than some reported molecular catalysts for electrochemical hydrogen production from neutral water. The TOF of a cobalt complex [32] in hydrogen production was only  $5 \text{ h}^{-1}$  at overpotential 390 mV. The turnover frequency for electrocatalytic water reduction was  $1010 \text{ s}^{-1}$  at 1.0 V (vs. Ag/AgCl) of cobalt corrole [15] and some molecular catalysts [33] such as Co-pentapyridine, molecular  $\text{MoS}_2$  catalyst, and Co-F8 were also lower than **2**. In summary, the performance of **2** for electrocatalytic hydrogen production is good in the homogeneous phase.

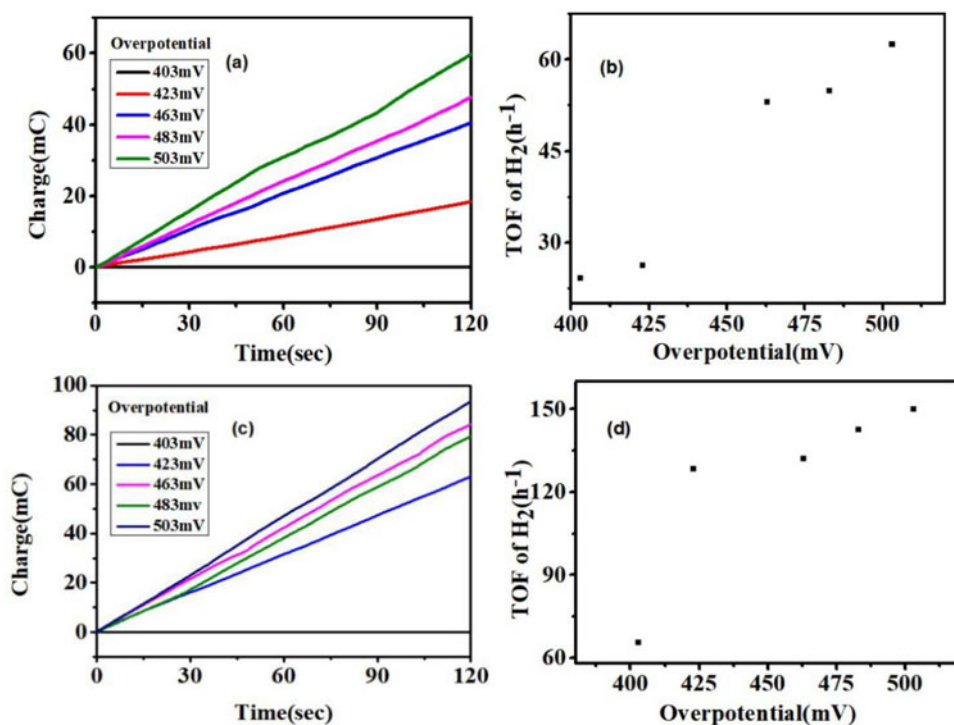


**Figure 5.** Charge buildup of **1** (a) and **2** (c) (0.005  $\mu\text{M}$ ) vs. different applied potentials in 0.25 M phosphate buffer at pH 7.0. All data have deducted the blank. Turnover frequency (mol  $\text{H}_2$ /mol catalysts/h) for electrocatalytic hydrogen production by **1** (b) and **2** (d) (0.005  $\mu\text{M}$ ) under different overpotentials (mV vs. SHE) in 0.25 M phosphate buffer (pH = 7.0).

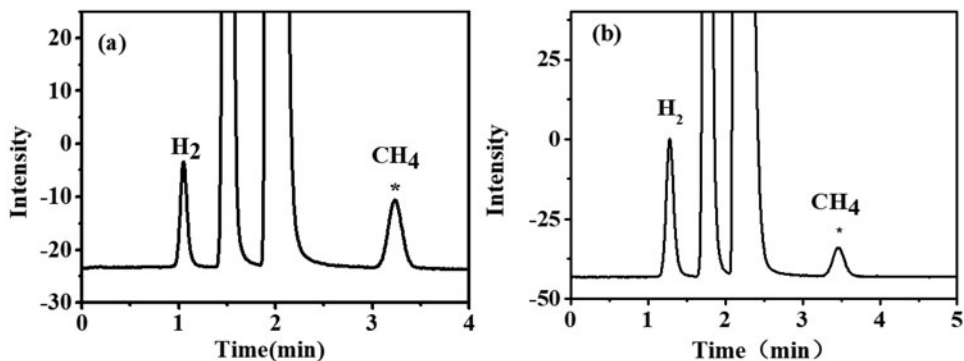


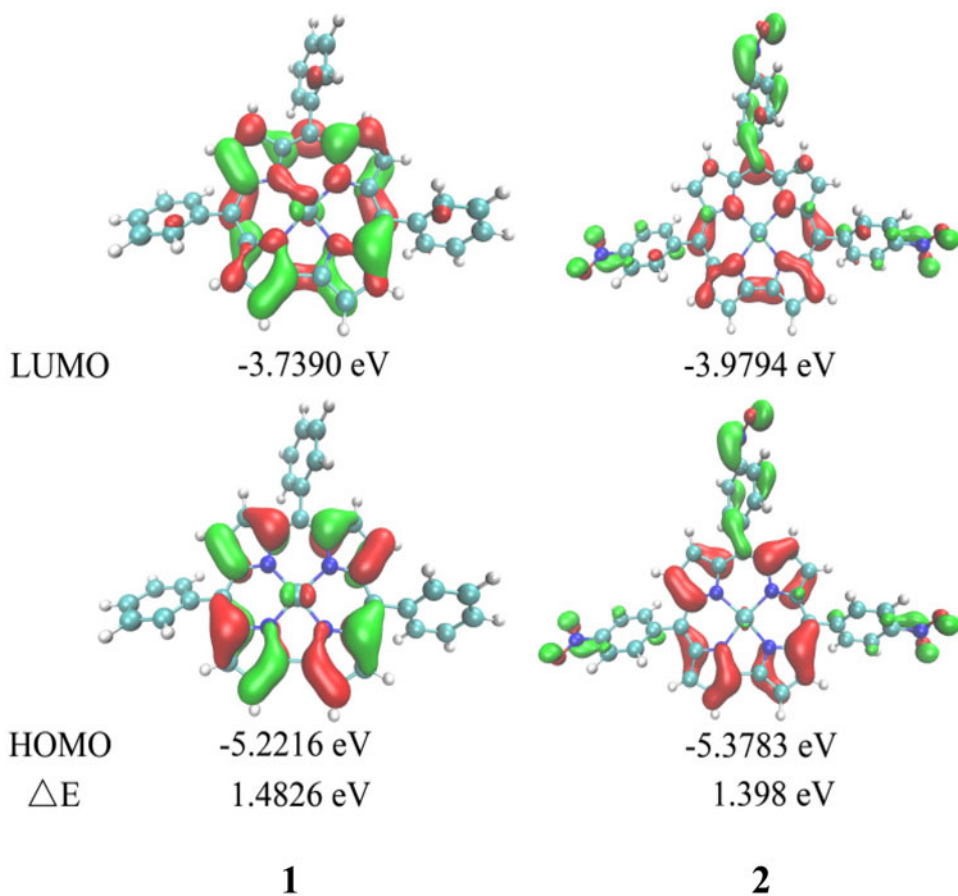
**Figure 6.** Complexes **1** (a) and **2** (b) GC traces after a 1 h controlled-potential electrolysis at  $-1.45\text{ V}$  vs.  $\text{Ag}/\text{AgCl}$  of 0.005  $\mu\text{M}$  complex **1** and **2** in 0.25 M phosphate buffer, pH 7.0. A standard of  $\text{CH}_4$  was added for calibration purposes.

From the CPE experiments, the maximum charge was only 98 mC under  $-1.45\text{ V}$  versus  $\text{Ag}/\text{AgCl}$  at pH 7.0 during 2 min of electrolysis in the absence of **1** (Supplementary material, Figure S6(a)). Upon addition of **1**, charge reached to 183.6 mC due to the formation of  $\text{H}_2$ . The evolved  $\text{H}_2$  was analyzed by gas chromatography. Complex **1** (Figure 6(a)) gave 0.26 mL of  $\text{H}_2$  over an electrolysis period of 1 h with a

Faradaic efficiency of 90.7% for H<sub>2</sub> and the TOF for **1** was 76 h<sup>-1</sup> under -1.45 V versus Ag/AgCl. Complex **2** (6b) gave 0.64 mL of H<sub>2</sub> over an electrolysis period of 1 h with a Faradaic efficiency of 91.8% for H<sub>2</sub> and the TOF for **2** was 188 h<sup>-1</sup> under -1.45 V versus Ag/AgCl.

### 3.4. Theoretical calculations

In order to explore the electronic structure of **1** and **2**, density functional theory (DFT) calculations were performed using the Gaussian 09 package [34]. The frontier molecular orbitals (FMOs) of **1** and **2** are shown in Scheme 3. The electron density of the highest occupied molecular orbital (HOMO) and lowest unoccupied molecular orbital (LUMO) were both distributed at the meso position as well as on the N atoms of pyrrole rings, whereas they shifted towards the NO<sub>2</sub> group when the para-hydrogen in the meso-substituted phenyl group of corrole was substituted by NO<sub>2</sub> group. The electron density of **2** has also decreased. This may be due to the stronger electronegativity of the NO<sub>2</sub> group, which increased the degree of electron migration to NO<sub>2</sub> and



**Scheme 3.** FMOs of **1** and **2** and the  $\Delta E$  of LUMO and HOMO of complex ( $\Delta E$  is the energy gap of LUMO-HOMO).

decreased the degree of electron overlap with other atoms. The push-pull effects observed in the DFT studies are in agreement with the experimental data (red shift and broadening of Soret band, alteration of redox potentials and HOMO-LUMO energy gaps). In addition, the energy gap of LUMO and HOMO followed the order  $1 > 2$ . Since the  $\Delta E$  of **2** is smaller than that of **1**, the ground state of **2** is easily excited. As a result, **2** is more active than **1** in each chemical reaction [35]. Combined with our experimental results, it can be seen that **2** is superior to **1** in the catalytic hydrogen production.

### 3.5. Catalytic stability of the complexes

To evaluate the catalytic durability of **1** and **2**, we also operated extended CPE in water while keeping the pH at 7.0 with 0.25 M buffer. A potential of  $-1.45$  V versus Ag/AgCl was employed for the measurement in order to ensure rapid turnover rate during the electrolysis. It was shown (Supplementary material, Figure S8(c)), the total of 415.1 C was passed for **2** during electrolysis. The catalyst affords a robust and essentially linear charge build up over time, with no substantial loss during 72 h, and the pH of the solution increased from 7.0 to 8.4, consistent with the accumulation of  $\text{OH}^-$  by water reduction. Figure S7(a,b) (Supplementary material) displays the catalytic charge and current for **1**.

## 4. Conclusion

The two trisphenylcorrole cobalt complexes, **1** and **2**, could be used as homogeneous catalysts for electrochemical hydrogen evolution by using water as the proton source. These complexes can electrocatalyze hydrogen evolution from acetic acid or aqueous media (pH 7.0). Interestingly, in the practical electrocatalytic hydrogen evolution experiment at  $-1.45$  V versus Ag/AgCl overpotential for 1 h, 0.26 and 0.64 mL hydrogen was produced for **1** and **2**, respectively, showing the attachment of nitro groups on the phenyl group impacts the performance of cobalt triphenylcorrole. The systematic investigation of the effect of electronic structure on the electrocatalytic activity of cobalt corrole in hydrogen evolution under the homogenous system continues in our laboratory.

## Disclosure statement

No potential conflict of interest was reported by the authors.

## Funding

This research was funded by the National Natural Science Foundation of China (Nos. 21671068, 21161001) and Science and Technology Plan of Jiangxi Provincial Department of Education (GJJ160941).

## References

- [1] L. Duan, L. Tong, Y. Xu, L. Sun. *Energy Environ. Sci.*, **4**, 3296 (2011).
- [2] V.S. Thoi, H.I. Karunadasa, Y. Surendranath, J.R. Long, C.J. Chang. *Energy Environ. Sci.*, **5**, 7762 (2012).
- [3] N.S. Lewis, D.G. Nocera. *Proc. Natl. Acad. Sci. USA.*, **103**, 15729 (2006).
- [4] J.R. McKone, S.C. Marinescu, B.S. Brunschwig, J.R. Winkler, H.B. Gray. *Chem. Sci.*, **5**, 865 (2014).
- [5] J.C. Fontecilla-Camps, A. Volbeda, C. Cavazza, Y. Nicolet. *Chem. Rev.*, **107**, 4273 (2007).
- [6] J.L. Dempsey, B.S. Brunschwig, J.R. Winkler, H.B. Gray. *Acc. Chem. Res.*, **42**, 1995 (2009).
- [7] G. Berggren, A. Adamska, C. Lambert, T.R. Simmons, J. Esselborn, M. Atta, S. Gambarelli, J.M. Mouesca, E. Reijerse, W. Lubitz, T. Happe, V. Artero, M. Fontecave. *Nature*, **499**, 66 (2013).
- [8] T. Fang, H.-X. Lu, J.-X. Zhao, S.-Z. Zhan, Q.-Y. Lv. *J. Mol. Catal. A. Chem.*, **396**, 304 (2015).
- [9] W.M. Singh, T. Baine, S. Kudo, S. Tian, X.A. Ma, H. Zhou, N.J. DeYonker, T.C. Pham, J.C. Bollinger, D.L. Baker, B. Yan, C.E. Webster, X. Zhao. *Angew. Chem. Int. Ed. Engl.*, **51**, 5941 (2012).
- [10] Z. Gross, L. Simkhovich, N. Galili. *Chem. Commun.*, **35**, 599 (1999).
- [11] L. Simkhovich, Z. Gross. *Tetrahedron Lett.*, **42**, 8089 (2001).
- [12] T. Kuwano, T. Kurahashi, S. Matsubara. *Chem. Lett.*, **42**, 1241 (2013).
- [13] W. Zhang, W. Lai, R. Cao. *Chem. Rev.*, **117**, 3717 (2017).
- [14] A. Mahammed, B. Mondal, A. Rana, A. Dey, Z. Gross. *Chem. Commun.*, **50**, 2725 (2014).
- [15] H. Lei, A. Han, F. Li, M. Zhang, Y. Han, P. Du, W. Lai, R. Cao. *Phys. Chem. Chem. Phys.*, **16**, 1883 (2014).
- [16] H. Lei, H. Fang, Y. Han, W. Lai, X. Fu, R. Cao. *ACS Catal.*, **5**, 5145 (2015).
- [17] H.-Q. Yuan, H.-H. Wang, J. Kandhadi, H. Wang, S.-Z. Zhan, H.-Y. Liu. *Appl. Organometal. Chem.*, **31**, e3773 (2017).
- [18] Z. Ou, A. Lu, D. Meng, S. Huang, Y. Fang, G. Lu, K.M. Kadish. *Inorg. Chem.*, **51**, 8890 (2012).
- [19] (a) B. Li, Z. Ou, D. Meng, J. Tang, Y. Fang, R. Liu, K.M. Kadish. *J. Inorg. Biochem.*, **136**, 130 (2014); (b) T. Ding, E.A. Alemán, D.A. Modarelli, C.J. Ziegler. *J. Phys. Chem. A*, **109**, 7411 (2005).
- [20] G. Lu, J. Li, X. Jiang, Z. Ou, K.M. Kadish. *Inorg. Chem.*, **54**, 9211 (2015).
- [21] R. Paolesse, S. Nardis, F. Sagone, R.G. Khoury. *J. Org. Chem.*, **66**, 550 (2001).
- [22] J. Fryxelius, G. Eilers, Y. Feyziyev, A. Magnuson, L. Sun, R. Lomoth. *J. Porphyrins Phthalocyanines*, **09**, 379 (2005).
- [23] D. Bhattacharya, P. Singh, S. Sarkar. *Inorg. Chim. Acta*, **363**, 4313 (2010).
- [24] P. Singh, I. Saltsman, A. Mahammed, I. Goldberg, B. Tumanskii, Z. Gross. *J. Porphyrins Phthalocyanines*, **16**, 663 (2012).
- [25] M.A. Morales Vásquez, M. Hamer, N.I. Neuman, A.Y. Tesio, A. Hunt, H. Bogo, E.J. Calvo, F. Doctorovich. *Chem. Cat. Chem*, **9**, 3259 (2017).
- [26] B. Kozarna, D.T. Gryko. *J. Org. Chem.*, **71**, 3707 (2006).
- [27] H.I. Karunadasa, C.J. Chang, J.R. Long. *Nature*, **464**, 1329 (2010).
- [28] X. Hu, B.S. Brunschwig, J.C. Peters. *J. Am. Chem. Soc.*, **129**, 8988 (2007).
- [29] S. Ganguly, D. Renz, L.J. Giles, K.J. Gagnon, L.J. McCormick, J. Conradie, R. Sarangi, A. Ghosh. *Inorg. Chem.*, **56**, 14788 (2017).
- [30] G.A.N. Felton, R.S. Glass, D.L. Lichtenberger, D.H. Evans. *Inorg. Chem.*, **45**, 9181 (2006).
- [31] H.I. Karunadasa, E. Montalvo, Y. Sun, M. Majda, J.R. Long, C.J. Chang. *Science*, **335**, 698 (2012).
- [32] P.V. Bernhardt, L.A. Jones. *Inorg. Chem.*, **38**, 5086 (1999).
- [33] B. Mondal, K. Sengupta, A. Rana, A. Mahammed, M. Botoshansky, S.G. Dey, Z. Gross, A. Dey. *Inorg. Chem.*, **52**, 3381 (2013).
- [34] M.J. Frisch, G.W. Trucks, H.B. Schlegel, G.E. Scuseria, M.A. Robb, J.R. Cheeseman, G. Scalmani, V. Barone, B. Mennucci, G.A. Petersson, H. Nakatsuji, M. Caricato, X. Li, H.P.

- Hratchian, A.F. Izmaylov, J. Bloino, G. Zheng, J.L. Sonnenberg, M. Hada, M. Ehara, K. Toyota, R. Fukuda, J. Hasegawa, M. Ishida, T. Nakajima, Y. Honda, O. Kitao, H. Nakai, T. Vreven, J.A. Montgomery, Jr., J.E. Peralta, F. Ogliaro, M. Bearpark, J.J. Heyd, E. Brothers, K.N. Kudin, V.N. Staroverov, T. Keith, R. Kobayashi, J. Normand, K. Raghavachari, A. Rendell, J.C. Burant, S.S. Iyengar, J. Tomasi, M. Cossi, N. Rega, J.M. Millam, M. Klene, J.E. Knox, J.B. Cross, V. Bakken, C. Adamo, J. Jaramillo, R. Gomperts, R.E. Stratmann, O. Yazyev, A.J. Austin, R. Cammi, C. Pomelli, J.W. Ochterski, R.L. Martin, K. Morokuma, V.G. Zakrzewski, G.A. Voth, P. Salvador, J.J. Dannenberg, S. Dapprich, A.D. Daniels, O. Farkas, J.B. Foresman, J.V. Ortiz, J. Cioslowski, D.J. Fox. *Gaussian 09, Revision D.01*, Gaussian, Inc., Wallingford, CT (2009).
- [35] N. Levy, A. Mahammed, M. Kosa, D.T. Major, Z. Gross, L. Elbaz. *Angew. Chem. Int. Ed. Engl.*, **54**, 14080 (2015).